

---

# RESTING NEURONS, ACTIVE INSIGHTS: IMPROVING INPUT SPARSIFICATION FOR LARGE LANGUAGE MODELS

---

**Haotian Xu**

Department of Applied Mathematics and Statistics  
Stony Brook University  
Stony Brook, NY 11794  
haotian.xu@stonybrook.edu

**Tian Gao**

Thomas J. Watson Research Center  
IBM Research  
Yorktown Heights, NY 10598  
tgao@us.ibm.com

**Tsui-Wei Weng**

Hacıoğlu Data Science Institute  
University of California, San Diego  
La Jolla, CA 92093  
lweng@ucsd.edu

**Tengfei Ma**

Department of Biomedical Informatics  
Stony Brook University  
Stony Brook, NY 11794  
tengfei.ma@stonybrookmedicine.edu

## ABSTRACT

Large Language Models (LLMs) achieve state-of-the-art performance across a wide range of applications, but their massive scale poses significant challenges for both efficiency and interpretability. Structural pruning, which reduces model size by removing redundant computational units such as neurons, has been widely explored as a solution, and this study devotes to input sparsification, an increasingly popular technique that improves efficiency by selectively activating only a subset of entry values for each input. However, existing approaches focus primarily on computational savings, often overlooking the representational consequences of sparsification and leaving a noticeable performance gap compared to full models. In this work, we first reinterpret input sparsification as a form of dynamic structural pruning. Motivated by the spontaneous baseline firing rates observed in biological neurons, we introduce a small set of trainable **spontaneous neurons** that act as compensatory units to stabilize activations in sparsified LLMs. Experiments demonstrate that these auxiliary neurons substantially reduce the sparsification-induced performance gap while generalizing effectively across tasks.

## 1 Introduction

Large Language Models (LLMs) have achieved state-of-the-art performance across a wide range of tasks [1, 2, 3, 4, 5], with scaling in model size and training data driving continuous improvements [6]. However, the massive parameter counts of modern LLMs present major obstacles for efficient deployment and mechanistic interpretability. These challenges are especially pronounced in latency-sensitive applications and edge-device deployments, where memory and compute budgets are limited. To mitigate this, pruning and sparsity techniques [7, 8, 9, 10, 11, 12, 13] reduce network size by eliminating redundant weights or activations, offering a promising and effective solution. Such approaches are typically data-independent and operate at different levels of granularity, including unstructured, semi-structured, and structured sparsity.

Beyond input-independent pruning, dynamic activation sparsity [14, 11, 10] provides an alternative path for accelerating inference without permanently compressing model parameters. These approaches enforce input-dependent structure on weight matrices by inducing sparsity in the hidden states. While conceptually attractive, existing methods [14, 15, 16] typically fail to achieve full sparsity and often require substantial additional pre-training to recover performance. To overcome these limitations, recent work has explored hybrid strategies that combine activation sparsity with magnitude-based pruning. For example, CATS [17] determines cutoff thresholds in MLP blocks via empirical histograms and zeros out sub-threshold activations; TEAL [10] extends this idea to all activations across both Attention and MLP blocks;

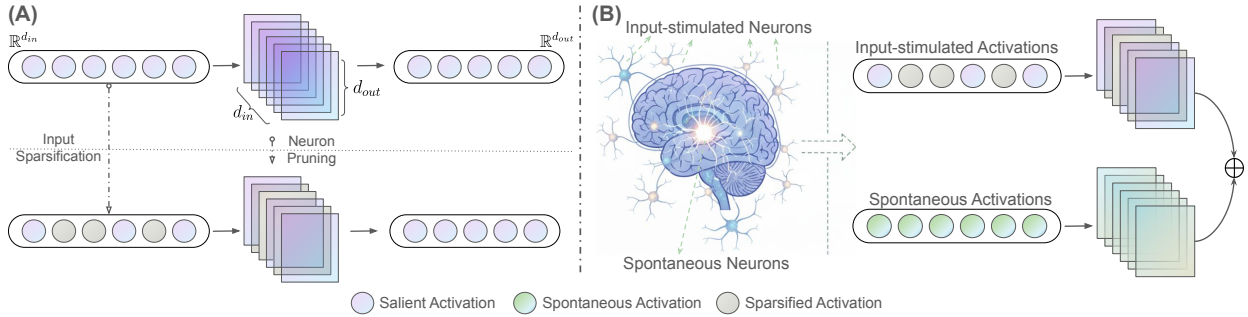


Figure 1: **Overview of Input Sparsification and Spontaneous Neurons.** (A) demonstrates that input sparsification thresholds low-magnitude activation entries to zero, eliminating the need to move the associated weight channels onto the registers. This is analogous to neuron pruning, enabling wall-clock speed-ups. (B) briefly demonstrates the concept of spontaneous neurons. These neurons can be reached by an input-independent activation with pre-trained neuron blocks.

LaRoSA [18] applies layerwise orthogonal rotations to transform activations into representations more amenable to sparsification; and R-Sparse [19] leverages channel and singular-value sparsity, removing the need for explicit active channel prediction as required in output-based sparsity approaches.

However, models with input sparsification still lag behind dense counterparts, exhibiting degraded performance across tasks and sparsity levels. The reason behind this problem might be due to the reduced pre-trained knowledge utilities as input sparsification selectively activates a subset of pre-trained neurons while abandoning the less significant ones. This suggests that dynamic pruning introduces representational instability or information loss, limiting practical adoption.

We address this challenge by introducing **spontaneous neurons**, a novel mechanism inspired by spontaneous activity in biological neural systems [20, 21, 22]. Our approach augments sparse computation with learnable, input-independent activations that act as representational scaffolds. These spontaneous neurons complement input-dependent selections, encoding prior expectations and preserving critical information. Crucially, they can be merged into bias terms after training, incurring no additional inference cost. We optimize them via knowledge distillation, minimizing KL divergence between dense and sparse model outputs.

By bridging neuroscientific principles with practical LLM optimization, we provide a principled framework for improving sparse inference. Our contributions are:

- We propose spontaneous neurons, a lightweight and neuro-scientifically inspired mechanism to address performance degradation in LLMs with dynamic input sparsity.
- We show that our method effectively closes the performance gap between sparse and dense models while incurring no extra inference overhead, making it a practical and efficient solution for real-world deployment.
- We conduct extensive experiments to demonstrate how spontaneous neurons stabilize model representations and provide a comprehensive analysis of their design, including optimal injection layers and seamless compatibility with quantization.

## 2 Spontaneous Neurons

In this section, we introduce our proposed method, *spontaneous neurons*, which aims to preserve the efficiency benefits of input sparsification methods while simultaneously improving the accuracy.

### 2.1 Preliminaries

We focus our analysis on the decoder layers of transformer-based LLMs, where each layer consists of attention heads and MLP blocks. Unlike prior works [11, 23] that primarily emphasize MLP blocks, we treat attention and MLP components uniformly, referring to them collectively as *blocks*.

In most LLMs, the forward pass of a block can be expressed as either a single linear mapping or a composition of linear mappings. For attention and MLP, the transformations are given by

$$Y = \text{softmax}\left(\frac{(\mathbf{W}_Q X)(\mathbf{W}_K X)^\top}{\sqrt{d}}\right) (\mathbf{W}_V X)^\top, \quad (1)$$

$$Y = \mathbf{W}X, \quad (2)$$

where  $X \in \mathbb{R}^{b \times k \times d_{in}}$  is the input representation,  $\mathbf{W} \in \mathbb{R}^{d_{in} \times d_{out}}$  are the trainable weight matrices, and  $Y \in \mathbb{R}^{b \times k \times d_{out}}$  is the output. Here,  $b$  denotes the batch size,  $k$  the input sequence length, and  $d_{in}, d_{out}$  the input and output dimensionalities, respectively.

With this setup, we now formalize input sparsification and show how it can be interpreted as dynamic, neuron-level pruning.

## 2.2 Input Sparsification as Dynamic Neuron Pruning

Since the attention operation defined in Equation 1 [24] is composed of multiple linear mappings, we begin by analyzing a single linear transformation for clarity. Consider the MLP formulation in Equation 2, which can be expanded as a linear combination over the column vectors of  $\mathbf{W}$ :

$$Y = \mathbf{W}X = \sum_{i=1}^{d_{in}} x_i \vec{w}_i, \quad (3)$$

where  $\vec{w}_i$  denotes the  $i$ -th column of  $\mathbf{W}$ . In this view, each input entry  $x_i$  controls the contribution, or activation strength, of the corresponding feature vector  $\vec{w}_i$  in the output. This is analogous to how a biological neuron modulates its firing rate in response to incoming electrical signals. Interestingly, Equation 3 also resembles the reconstruction step in a sparse autoencoder (SAE) [25], where the basis vectors  $\vec{w}_i$  can be interpreted as concept features.

Input sparsification [26, 27, 28, 29] modifies this computation by suppressing contributions below a certain threshold. Specifically, a heuristic or learned criterion determines which entries are retained, giving

$$Y = \sum_{i=1}^{d_{in}} \mathbf{I}[x_i > \tau] x_i \vec{w}_i, \quad (4)$$

where  $\mathbf{I}[x_i > \tau]$  is an indicator function that outputs 1 if  $x_i > \tau$  and 0 otherwise. Effectively, this masks out the contributions of  $\vec{w}_i$  whose activations fall below the threshold, as illustrated in Figure 1.

Viewed this way, input sparsification is mathematically equivalent to pruning certain neurons in an LLM, with the key distinction that the pruning decision depends on the input. Hence, it can be naturally interpreted as a form of *dynamic neuron pruning*. In Appendix A, we also briefly discuss about the related but simpler approaches of a fixed neuron pruning or fixed structural pruning compared to unstructural pruning.

## 2.3 Baseline Firing Rates

Recent evidence suggests that LLMs share intriguing parallels with biological neural systems, particularly in their sparse and selective internal activations [30, 31, 32, 33, 34]. Neuroscience has long established that concepts are encoded by sparse ensembles of neurons, with individual cells responding selectively to high-level entities such as specific people or objects [35, 36, 37, 38]. This sparse coding mechanism enables robust and efficient representations while avoiding redundancy [39, 40]. Inspired by this observation, recent work on *input sparsification* in LLMs [26, 27, 28, 29] has proposed activating only a subset of neurons per input, thereby reducing computational cost while preserving much of the pretrained knowledge. Unlike static structural pruning [10, 18, 41, 42, 43], this adaptive strategy retains greater representational flexibility and aligns more closely with biological sparsity.

Despite these benefits, a critical limitation remains. Different inputs tend to activate largely disjoint subsets of neurons, and there is no small set of neurons consistently active across diverse inputs. This heterogeneity implies the absence of a universal *prior expectation*—a baseline activity that could anchor representations and provide continuity, much like how biological systems compare new sensory information against existing internal states.

In neuroscience, such stability is achieved through *spontaneous activity*, where neurons fire even in the absence of external stimuli [20, 21, 22]. These baseline firing patterns encode prior expectations and maintain network readiness for incoming information. Motivated by this principle, we propose introducing a small set of consistently active units in LLMs, which we call *spontaneous neurons*. These neurons act as static scaffolds, preserving essential representational

capacity and complementing dynamically activated neurons under sparsification. Conceptually, spontaneous neurons distill knowledge from the full dense model into lightweight static representations, which—when combined with input-dependent activations—yield a closer approximation to the behavior of the original model.

## 2.4 Details of Spontaneous Neurons

In neuroscience, *spontaneous activity* refers to the baseline firing of neurons in the absence of explicit sensory input [20, 21, 22, 44, 45]. Such activity is believed to encode prior expectations and to prepare neural circuits for rapid responses to incoming stimuli. Inspired by this phenomenon, we model spontaneous activity in LLMs as a set of universal activation vectors that are added to each block, independent of the input. Formally, we write:

$$Y = \mathbf{W} \cdot \mathbf{S}(X) + \mathbf{W} \cdot \vec{\alpha}, \quad (5)$$

where  $\mathbf{S}(\cdot)$  denotes the input sparsification function acting on input  $X$ , and  $\vec{\alpha}$  represents the static spontaneous activation vector. Since  $\vec{\alpha}$  does not depend on  $X$ , the term  $\mathbf{W} \cdot \vec{\alpha}$  can be equivalently absorbed into a learnable bias vector  $\vec{b}$  after training, thereby eliminating the need for additional matrix multiplications at inference time.

To learn  $\vec{\alpha}$ , we align the behavior of the sparse model with that of the full model. Specifically, we use a calibration dataset and optimize  $\vec{\alpha}$  by minimizing the KL divergence between the output distributions of the full dense model and those of the sparse model augmented with spontaneous neurons:

$$\mathcal{L} = \text{KL}(f(X), f(\mathbf{S}(X); \vec{\alpha})), \quad (6)$$

where  $f(\cdot)$  denotes the function computed by the LLM backbone. Intuitively, this objective distills the full model’s predictive distribution into the spontaneous neurons, enabling them to encode a form of prior expectation that complements the dynamically selected neurons.

By integrating spontaneous neurons, we aim to preserve the efficiency benefits of input sparsification while compensating for its performance degradation, thereby providing a principled and biologically inspired mechanism for stable sparse inference in LLMs.

## 2.5 Spontaneous Neurons Theoretically Reduce Approximation Errors

Consider a dense layer  $Y = \mathbf{W}X$  and its sparse approximation  $\hat{Y}_0 = \mathbf{W}S(X)$ , where  $S(\cdot)$  selects a subset of input features. Directly using  $\mathbf{W}S(X)$  introduces a residual error  $e(X) = \mathbf{W}X - \mathbf{W}S(X)$ , which may accumulate across layers. Augmenting with the spontaneous neurons brings in a bias term and yields  $\hat{Y}_b = \mathbf{W}S(X) + \vec{b}$ .

If  $b$  is input-dependent, it can exactly recover the dense output, i.e.,  $\hat{Y}_b = \mathbf{W}X$ . Even when restricted to a constant bias vector, the optimal choice is  $b^* = \mathbb{E}[e(X)]$ , which cancels the average residual shift. Consequently, the **expected approximation error** satisfies

$$\mathcal{L}(b^*) = \mathbb{E} [\|e(X) - b\|^2] \leq \mathcal{L}(0) = \mathbb{E} [\|e(X)\|^2], \quad (7)$$

with strict improvement unless the residual mean vanishes.

Intuitively, the bias term acts as a correction that absorbs systematic error introduced by sparsification. Our *spontaneous neurons* realize this correction in a learnable and data-driven way: they encode stable baseline activations that compensate for missing features and stabilize sparse inference. Detailed derivations are provided in the Appendix B.1.

# 3 Experiments and Analyses

In this section, we will discuss about our experiment settings, results, and their possible enlightenment for future designing and understanding LLMs.

## 3.1 Models, Datasets, & Baselines

We evaluate spontaneous neurons on three widely used LLMs—Llama3-8B [5], Qwen3-8B [46], and Mistral-v2-7B [47]—and further include Llama3-1B to examine effects on smaller models. Wikitext [48] serves both as calibration data for training spontaneous neurons and as a benchmark for language modeling performance, measured by perplexity. To assess zero-shot generalization, we adopt six downstream tasks from EleutherAI LM Harness [49]: CommonsenseQA [50], TruthfulQA [51], OpenBookQA [52], MedMCQA [53], MMLU [54, 55], and MathQA [56]. For all QA tasks, we report mean accuracy. Implementation details are provided in Appendix C.

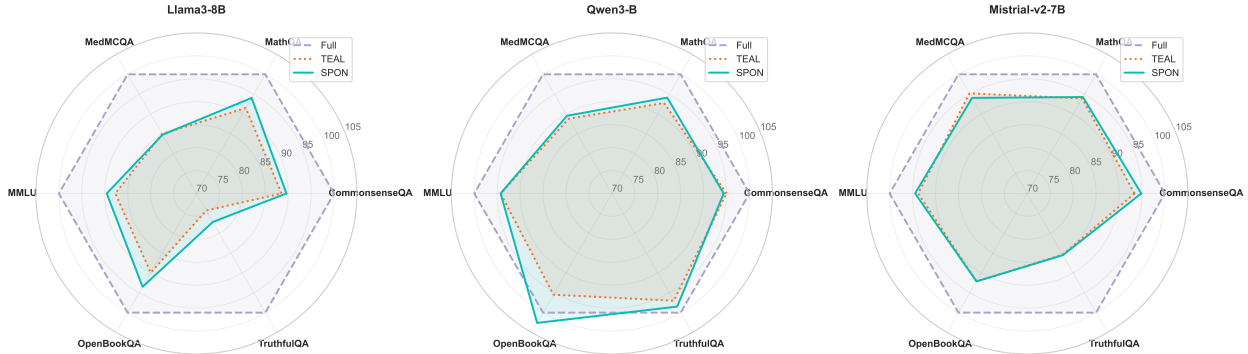


Figure 2: Comparing TEAL and SPON on general and mathematical reasoning. We report normalized mean accuracy. Each point in the radar capability charts is (sparse performance)/(dense performance).

Table 1: Perplexity results on language modeling task. Spontaneous Neurons help to approximate the original full model’s performance across different sparsity levels and heterogeneous backbone models.

Method	Sparsity	Language Modeling			
		Llama3-1B	Llama3-8B	Qwen3-8B	Mistral-v2-7B
Full	0%	12.14	6.75	8.99	5.49
Wanda	50%	29.68	9.66	10.41	6.26
Fixed Neuron Pruning	50%	62.36	-	-	-
TEAL	25%	-	6.88	9.04	5.52
SPON	25%	-	6.92	8.94	5.58
TEAL	50%	17.03	8.34	9.75	6.00
SPON	50%	15.43	7.83	9.26	5.86
TEAL	60%	-	11.62	11.38	6.90
SPON	60%	-	9.63	10.42	6.51

Since spontaneous neurons build on input sparsification, we compare against methods in this domain, including CATS [17] and TEAL [10], using TEAL and the dense model as our primary baselines. We also include Wanda [7], a state-of-the-art unstructured pruning method, and a simple fixed neuron pruning strategy. Appendix A further analyzes why fixed structural pruning underperforms unstructured pruning, supporting our focus on dynamic neuron pruning.

### 3.2 Spontaneous Neurons Improve Language Modeling

**Main Results.** As shown in Table 1, SPON demonstrates strong performance across different sparsity levels. At moderate sparsity (25%), the degradation in perplexity is negligible, aligning with prior observations from TEAL experiments [10] that LLMs can tolerate a significant degree of sparsification without losing accuracy. When pursuing more aggressive sparsity for greater inference efficiency, however, we observe that TEAL alone begins to suffer substantial performance degradation, especially beyond the 50% threshold where task understanding and generalization ability sharply deteriorate across all three backbone models. In these high-sparsity regimes, introducing spontaneous neurons (SPON) consistently mitigates the degradation. This improvement is particularly evident for newer backbones such as Llama3-8B and Qwen3-8B, which are more vulnerable to performance collapse under heavy sparsification. In such cases, SPON not only stabilizes the model’s capacity but also provides a simple and effective way to retain language modeling ability, complementing recent findings that modern models are increasingly resistant to quantization techniques [57].

We further compare SPON with Wanda [7], a state-of-the-art unstructured pruning method, in contrast to TEAL/SPON, which represent dynamic structural pruning approaches. As discussed in Appendix A, structural pruning can be interpreted as imposing a low-rank projection on the original learned weight matrix, while unstructured pruning like Wanda preserves the rank and therefore tends to yield performance closer to the full dense model, explaining why Wanda substantially outperforms fixed neuron pruning in Table 1. However, by integrating spontaneous neurons, SPON enables structurally pruned models to sustain performance levels comparable to unstructured pruning, even at higher

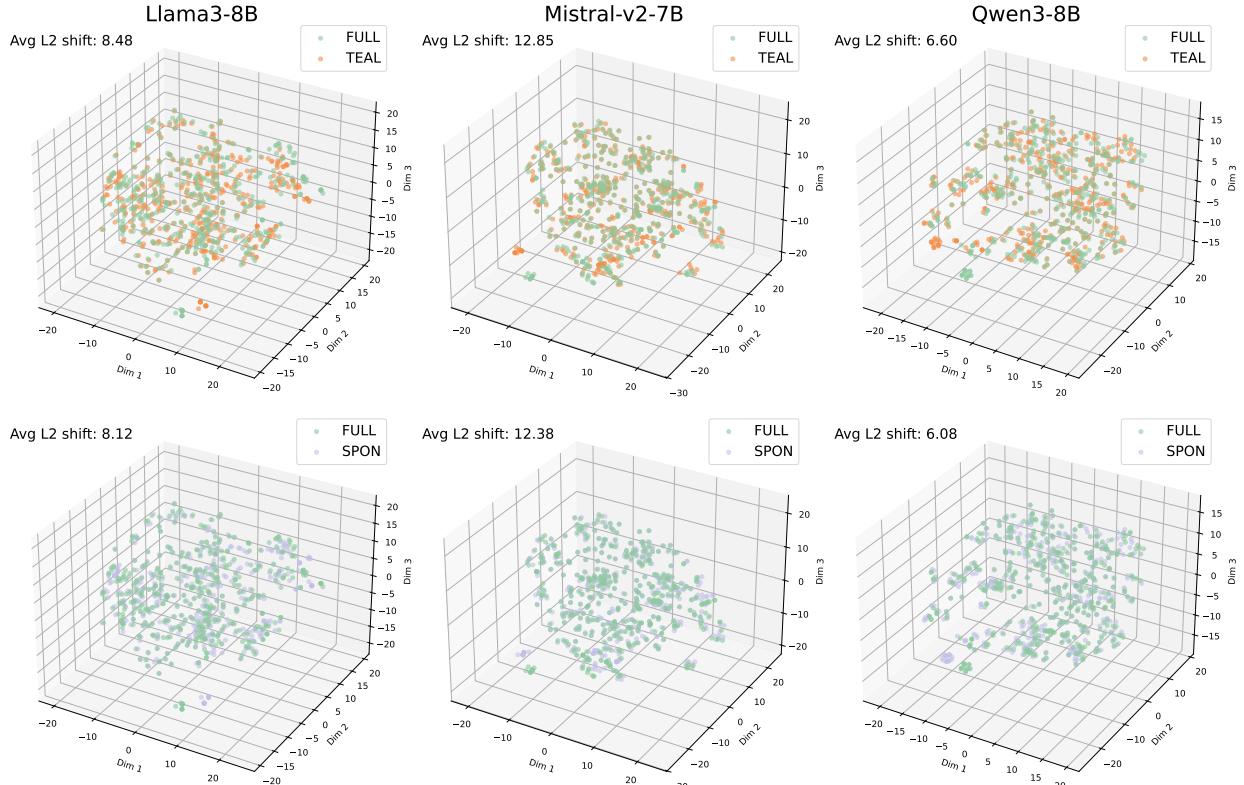


Figure 3: The distribution of hidden representations of TEAL and SPON after dimensionality reduction, where SPON consistently exhibits relatively smaller shift.

sparsity. These findings underscore the effectiveness of spontaneous neurons as a lightweight yet powerful mechanism to preserve model capacity and generalization under extreme sparsification.

### 3.3 Spontaneous Neurons Preserve Pretrained Knowledge

To better understand which specific capabilities are impacted by spontaneous neurons, we evaluate the major backbone models with its TEAL counterparts on several language model evaluation benchmarks. We select size tasks spanning different categories including math, medical, truthfulness, and etc. In Figure 2, we show the normalized mean accuracies (pruned model accuracy divided by full model accuracy) on 6 zero-shot task of pruned Llama3-8B, Mistral-v2-7B, and Qwen3-8B models. We refer the reader to Appendix D for task-wise numerical performance. Across different backbones and task domains, SPON, abbreviation for spontaneous neurons, exhibit a stable advantages over the well-established TEAL approach by a noticeable margin (especially in Llama3-8B and Qwen3-8B).

Our findings reveal that when just a small fraction of extra spontaneous neurons (in our case, we only need to have a single spontaneous neuron) are injected, the model’s performance on complex tasks involving general reasoning and mathematical understanding is significantly impacted under input sparsification. This is interestingly unexpected and even somehow contrary to modern LLM design, as the prevailing view is that when models are sufficiently large, the bias term does not play a particularly significant role [58, 59].

### 3.4 Hidden Representation Analysis

Input sparsification needs to mask some activation entries for each token and make a inevitable shift in the distribution of hidden representations. Hence, we aim to empirically verify that adding a spontaneous neuron can avoid such a distributional mismatch. To validate it, we conducted the following steps: i) we randomly select 50 prompts from wikitext-raw-v2 test set [48] (each prompt may have 64 token maximally, which results in more than 1000 tokens in end) and extract the hidden representation within the full LLMs and TEAL sparse one. ii) Subsequently, we performed the same operation on the sparse LLM with spontaneous neurons. iii) Finally, we used t-SNE [60] to visualize the hidden

representation distributions. Furthermore, we quantify the deviation of scatter point distributions and numerically exhibit the distributional shifts in Figure 3. From Figure 3, we can observe that

- **Having input sparsification can cause the hidden representation shifts.** This discrepancy becomes more pronounced for tokens locating on the periphery.
- **Adding spontaneous neurons help to maintain consistency in hidden representations.** Specifically, the hidden representations within input-sparsification LLMs using spontaneous neurons remain consistent with the original distribution across all three base models. This stability indicates that injecting spontaneous effectively mitigates the underlying distribution shift, in turn explaining its superior knowledge preservation and generalization capabilities.

### 3.5 Latency

Table 2: Having the spontaneous neuron can preserve the high inference efficiency.

Method	TPS	
	Llama3-8B	Mistral-v2-7B
FULL (0%)	42.648	44.173
TEAL (50%)	64.279	71.246
SPON (50%)	64.131	71.836

For measure the inference efficiency, we adopt the same setting introduced in TEAL [10]. We benchmark TEAL’s and SPON’s end-to-end single-batch decoding latency by integrating it with GPT-Fast (PyTorch, 2024). We enable CUDA graphs and torch.compile. Tests use three models Llama3-8B, Mistral-v2-7B, and Qwen3-8B models at 50% uniform sparsities. We do the experiment on single A6000 GPU setting, and our GPU power limit setting is 300W . As shown in Table 2, TEAL achieves significant speed-ups of up to 1.5x and 1.6x at 50% sparsity for Llama3-8B and Mistral-v2-7B respectively. The Table 2 also indicates that storing the spontaneous neuron as the bias term will not impact the inference speed.

The spontaneous neuron is simply added as a small bias term in each linear layer. Since the main cost of a linear layer comes from the large matrix multiplication, this extra bias addition is almost free in practice. The extra computation is marginal, and the number of new parameters is tiny because we only add one small vector per layer. In other words, spontaneous neurons give us new modeling flexibility while keeping the inference speed and memory usage essentially unchanged.

### 3.6 Where to Inject Spontaneous Neurons

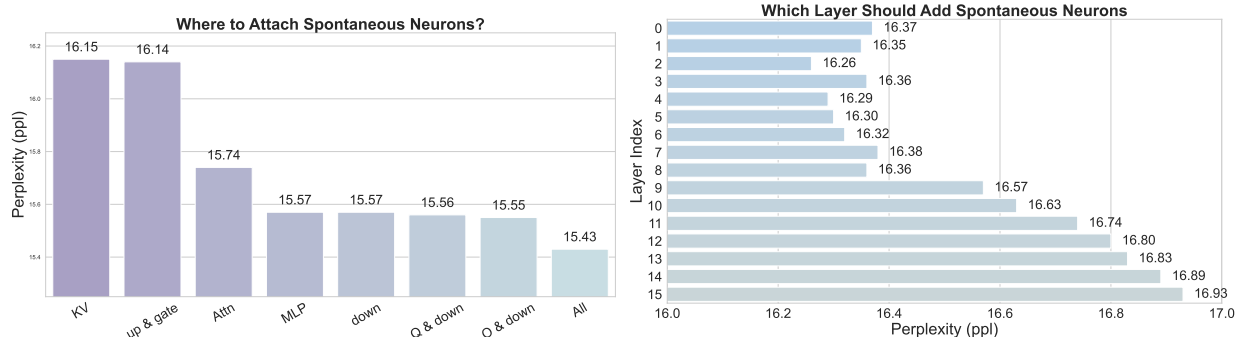


Figure 4: Left: We show that only injecting extra spontaneous neurons in down projection of MLP module can be comparable as injecting them to each block; Right: We continue to investigate which layer favors more about the spontaneous neurons.

In the previous sections, we demonstrated the effectiveness of spontaneous neurons on both in-domain language modeling tasks and several out-of-domain QA benchmarks. We also showed that their efficiency is preserved by absorbing them into bias terms at inference, and provided mathematical and visual analyses that motivate their benefit for sparse inference.

In this subsection, we take a more engineering-oriented perspective: *which components of the model benefit most from additional spontaneous neurons?* We conduct experiments on Llama3-1B with WikiText, using perplexity as the evaluation metric.

As illustrated in Figure 4, we examine the following candidate locations for attaching spontaneous neurons:

- Key–Value projections in Attention,
- Up and gate projections in MLP,
- Query projection in Attention + down projection in MLP,
- Output projection in Attention + down projection in MLP,
- Down projection in MLP only.

The results indicate that MLP layers benefit more from spontaneous neurons than Attention layers. For instance, injecting spontaneous neurons exclusively into MLP blocks achieves a perplexity of 15.57, compared to 15.74 when applied to Attention blocks only. Moreover, within the MLP, different operations show varying sensitivity: the *down projection* consistently emerges as the most effective site. Injecting spontaneous neurons solely into the MLP down projection yields performance comparable to more complex configurations, making it the most efficient and impactful location for augmentation.

Beyond identifying which blocks benefit most, we also investigate the influence of *layer index*. Using Llama3-1B with WikiText as calibration data, we attach spontaneous neurons to the MLP down projection of a single layer at a time. Figure 4 shows that top layers (closer to the embedding layer) exhibit larger gains than bottom layers. This trend aligns with prior findings [61, 62, 63, 64], which suggest that upper layers capture local representations while lower layers specialize for final output generation.

Taken together, these observations suggest that spontaneous neurons likely distill part of the pretrained model knowledge into a small set of additional parameters. This provides stable prior expectations that enhance sparse inference, enabling compressed models to better approximate their dense counterparts.

### 3.7 Compatibility with Quantization

We further examine the compatibility of spontaneous neurons with quantization, another promising direction for efficient LLM inference. Specifically, we evaluate 32-bit and 16-bit floating-point formats in PyTorch, as well as 8-bit and 4-bit quantization using `bitsandbytes`. Figure 5 reports the perplexity results on WikiText for Llama3-8B, Mistral-v2-7B, and Qwen3-8B at 50% sparsity.

Across different quantization precisions, spontaneous neurons exhibit stable behavior without significant fluctuations in perplexity. Notably, even under `int4` quantization, our proposed architecture continues to outperform the numerical results reported for TEAL (Table 1) at the same sparsity level, which were measured under the 32-bit setting.

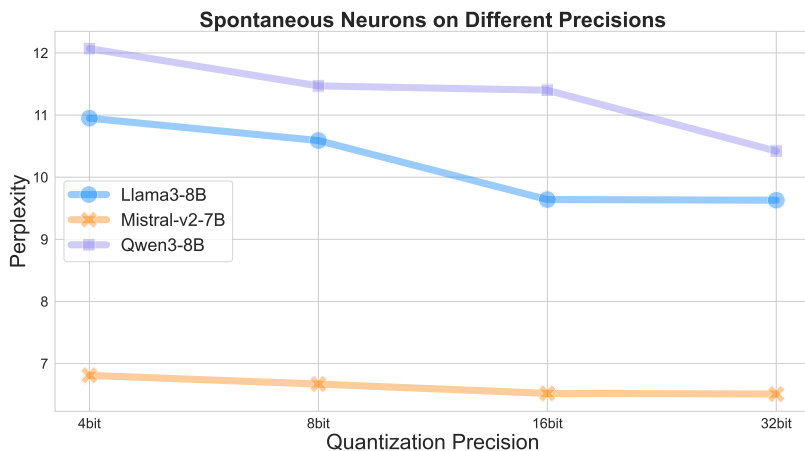


Figure 5: Perplexity for three different LLM backbones quantized to various bitwidths on WikiText. The sparsity ratio is chosen at a 50% level.

These findings suggest that combining activation sparsity and spontaneous neurons with weight quantization opens new regimes of efficiency by reducing memory traffic to GPU registers, thereby enabling faster inference. Realizing this potential, however, requires the development of specialized kernels that jointly support sparsity and quantization, which we leave as future work.

## 4 Other Related Work

### 4.1 Efficient LLM Inference through Model Pruning

Large Language Models (LLMs) are computationally and memory intensive at inference time, partly due to their massive parameter counts and the associated key–value (KV) cache storage. To address this, a variety of efficiency techniques have been developed, including pruning redundant components from the network [8, 7, 12, 13, 65, 66, 67, 9]

and distilling knowledge into smaller or more efficient architectures [68, 69, 70]. Our proposed approach can be seen as a hybrid of these two perspectives: by introducing lightweight spontaneous neurons, we implicitly distill part of the pretrained knowledge from the full dense model into a compact auxiliary structure, while maintaining the benefits of sparsity-based pruning.

## 4.2 Dynamic Inference with Activation Sparsity

Recent studies highlight that LLMs naturally exhibit significant activation sparsity, where a large fraction of hidden states are zero-valued. This phenomenon, also referred to as conditional computation, has long been observed in ReLU-based MLPs [26], and has motivated efforts to reintroduce activation sparsity into modern Transformer architectures. For example, replacing SiLU or GeLU activations with ReLU and continuing large-scale pretraining has been shown to recover competitive performance [16, 15], while Squared ReLU [71] has also emerged as an effective alternative. From a systems perspective, activation sparsity offers hardware advantages: it reduces GPU register transfers [72], and CPU offloading of sparse channels can further cut memory traffic between CPU and GPU [73].

Several recent approaches explicitly leverage this property. CATS introduces training-free activation sparsity for SwiGLU-based LLMs by pruning the magnitude of  $\mathbf{W}_{\text{gate}}$ , achieving up to 50% sparsity in  $\mathbf{W}_{\text{up}}$  and  $\mathbf{W}_{\text{down}}$  within MLP blocks [17]. R-Sparse [19] demonstrates that both attention and MLP layers can sustain high sparsity levels without significant performance loss, enabling deployment on edge devices. LaRoSA [18] applies layerwise orthogonal rotations, making activations more amenable to Top-K pruning, which yields consistent sparsity and reliable wall-clock acceleration. TEAL [10], in contrast, adopts a simple training-free magnitude-based pruning of hidden states across the model. Due to its conceptual simplicity and interpretability, we adopt TEAL as our primary baseline.

While these methods focus primarily on computational savings, they often neglect the representational degradation induced by input sparsification. Our work aims to complement these approaches by preserving the efficiency gains of activation sparsity while recovering the lost representational capacity. Conceptually, our proposed spontaneous neurons are orthogonal to existing techniques such as LaRoSA and R-Sparse, and can be integrated with them to further improve the trade-off between efficiency and accuracy.

## 5 Conclusion

We introduced *spontaneous neurons*, a simple and effective approach to mitigate the performance gap caused by input activation sparsity in LLMs. Our method integrates magnitude-based sparsification with a small set of trainable neurons that serve as prior activations, enabling models to achieve 50–60% sparsity with minimal degradation. Experiments demonstrate that spontaneous neurons consistently improve language modeling performance and zero-shot generalization across domains. Importantly, by folding spontaneous activations into bias terms at inference time, our approach incurs negligible computational overhead. We believe spontaneous neurons open new directions for sparse model design, and future work will explore spontaneous neurons in both pretraining and post-training regimes.

## References

- [1] Josh Achiam, Steven Adler, Sandhini Agarwal, Lama Ahmad, Ilge Akkaya, Florencia Leoni Aleman, Diogo Almeida, Janko Altenschmidt, Sam Altman, Shyamal Anadkat, et al. Gpt-4 technical report. *arXiv preprint arXiv:2303.08774*, 2023.
- [2] Anthropic. The claude 3 model family: Opus, sonnet, haiku.
- [3] Daya Guo, Dejian Yang, Haowei Zhang, Junxiao Song, Ruoyu Zhang, Runxin Xu, Qihao Zhu, Shirong Ma, Peiyi Wang, Xiao Bi, et al. Deepseek-r1: Incentivizing reasoning capability in llms via reinforcement learning. *arXiv preprint arXiv:2501.12948*, 2025.
- [4] Jinze Bai, Shuai Bai, Yunfei Chu, Zeyu Cui, Kai Dang, Xiaodong Deng, Yang Fan, Wenbin Ge, Yu Han, Fei Huang, et al. Qwen technical report. *arXiv preprint arXiv:2309.16609*, 2023.
- [5] Abhimanyu Dubey, Abhinav Jauhri, Abhinav Pandey, Abhishek Kadian, Ahmad Al-Dahle, Aiesha Letman, Akhil Mathur, Alan Schelten, Amy Yang, Angela Fan, et al. The llama 3 herd of models. *arXiv e-prints*, pages arXiv–2407, 2024.
- [6] Tom Brown, Benjamin Mann, Nick Ryder, Melanie Subbiah, Jared D Kaplan, Prafulla Dhariwal, Arvind Nee-lakantan, Pranav Shyam, Girish Sastry, Amanda Askell, et al. Language models are few-shot learners. *Advances in neural information processing systems*, 33:1877–1901, 2020.

- [7] Mingjie Sun, Zhuang Liu, Anna Bair, and J Zico Kolter. A simple and effective pruning approach for large language models. *arXiv preprint arXiv:2306.11695*, 2023.
- [8] Elias Frantar and Dan Alistarh. Sparsegpt: Massive language models can be accurately pruned in one-shot. In *International conference on machine learning*, pages 10323–10337. PMLR, 2023.
- [9] Shashata Sawmya, Linghao Kong, Ilya Markov, Dan Alistarh, and Nir Shavit. Wasserstein distances, neuronal entanglement, and sparsity. *arXiv preprint arXiv:2405.15756*, 2024.
- [10] James Liu, Pragaash Ponnusamy, Tianle Cai, Han Guo, Yoon Kim, and Ben Athiwaratkun. Training-free activation sparsity in large language models. *arXiv preprint arXiv:2408.14690*, 2024.
- [11] Qinsi Wang, Saeed Vahidian, Hancheng Ye, Jianyang Gu, Jianyi Zhang, and Yiran Chen. Coreinfer: Accelerating large language model inference with semantics-inspired adaptive sparse activation, 2024.
- [12] Lu Yin, You Wu, Zhenyu Zhang, Cheng-Yu Hsieh, Yaqing Wang, Yiling Jia, Gen Li, Ajay Jaiswal, Mykola Pechenizkiy, Yi Liang, et al. Outlier weighed layerwise sparsity (owl): A missing secret sauce for pruning llms to high sparsity. *arXiv preprint arXiv:2310.05175*, 2023.
- [13] Xinyin Ma, Gongfan Fang, and Xinchao Wang. Llm-pruner: On the structural pruning of large language models. *Advances in neural information processing systems*, 36:21702–21720, 2023.
- [14] Zichang Liu, Jue Wang, Tri Dao, Tianyi Zhou, Binhang Yuan, Zhao Song, Anshumali Shrivastava, Ce Zhang, Yuandong Tian, Christopher Re, et al. Deja vu: Contextual sparsity for efficient llms at inference time. In *International Conference on Machine Learning*, pages 22137–22176. PMLR, 2023.
- [15] Iman Mirzadeh, Keivan Alizadeh, Sachin Mehta, Carlo C Del Mundo, Oncel Tuzel, Golnoosh Samei, Mohammad Rastegari, and Mehrdad Farajtabar. Relu strikes back: Exploiting activation sparsity in large language models. *arXiv preprint arXiv:2310.04564*, 2023.
- [16] Zhengyan Zhang, Yixin Song, Guanghui Yu, Xu Han, Yankai Lin, Chaojun Xiao, Chenyang Song, Zhiyuan Liu, Zeyu Mi, and Maosong Sun. ReLU<sup>2</sup> wins: Discovering efficient activation functions for sparse llms. *arXiv preprint arXiv:2402.03804*, 2024.
- [17] Donghyun Lee, Je-Yong Lee, Genghan Zhang, Mo Tiwari, and Azalia Mirhoseini. Cats: Contextually-aware thresholding for sparsity in large language models. *arXiv preprint arXiv:2404.08763*, 2024.
- [18] Kai Liu, Bowen Xu, Shaoyu Wu, Xin Chen, Hao Zhou, Yongliang Tao, and Lulu Hu. La rosa: Enhancing llm efficiency via layerwise rotated sparse activation. *arXiv preprint arXiv:2507.01299*, 2025.
- [19] Zhenyu Zhang, Zechun Liu, Yuandong Tian, Harshit Khaitan, Zhangyang Wang, and Steven Li. R-sparse: Rank-aware activation sparsity for efficient llm inference. In *The Thirteenth International Conference on Learning Representations*.
- [20] David H Hubel and Torsten N Wiesel. Receptive fields, binocular interaction and functional architecture in the cat’s visual cortex. *The Journal of physiology*, 160(1):106, 1962.
- [21] Amos Arieli, Alexander Sterkin, Amiram Grinvald, and AD Aertsen. Dynamics of ongoing activity: explanation of the large variability in evoked cortical responses. *Science*, 273(5283):1868–1871, 1996.
- [22] Tal Kenet, Dmitri Bibitchkov, Misha Tsodyks, Amiram Grinvald, and Amos Arieli. Spontaneously emerging cortical representations of visual attributes. *Nature*, 425(6961):954–956, 2003.
- [23] Qinsi Wang, Hancheng Ye, Ming-Yu Chung, Yudong Liu, Yueqian Lin, Martin Kuo, Mingyuan Ma, Jianyi Zhang, and Yiran Chen. Corematching: A co-adaptive sparse inference framework with token and neuron pruning for comprehensive acceleration of vision-language models, 2025.
- [24] Ashish Vaswani, Noam Shazeer, Niki Parmar, Jakob Uszkoreit, Llion Jones, Aidan N Gomez, Łukasz Kaiser, and Illia Polosukhin. Attention is all you need. *Advances in neural information processing systems*, 30, 2017.
- [25] Hoagy Cunningham, Aidan Ewart, Logan Riggs, Robert Huben, and Lee Sharkey. Sparse autoencoders find highly interpretable features in language models. *arXiv preprint arXiv:2309.08600*, 2023.
- [26] Zonglin Li, Chong You, Srinadh Bhojanapalli, Daliang Li, Ankit Singh Rawat, Sashank J Reddi, Ke Ye, Felix Chern, Felix Yu, Ruiqi Guo, et al. The lazy neuron phenomenon: On emergence of activation sparsity in transformers. *arXiv preprint arXiv:2210.06313*, 2022.
- [27] Zhenyu Zhang, Zechun Liu, Yuandong Tian, Harshit Khaitan, Zhangyang Wang, and Steven Li. R-sparse: Rank-aware activation sparsity for efficient llm inference. *arXiv preprint arXiv:2504.19449*, 2025.
- [28] Yuqi Luo, Chenyang Song, Xu Han, Yingfa Chen, Chaojun Xiao, Xiaojun Meng, Liqun Deng, Jiansheng Wei, Zhiyuan Liu, and Maosong Sun. Sparsing law: Towards large language models with greater activation sparsity. *arXiv preprint arXiv:2411.02335*, 2024.

- [29] Romain Storai, Jaeseong Lee, and Seung-won Hwang. Smarter, not harder: Training-free adaptive computation for transformers. In *Findings of the Association for Computational Linguistics: ACL 2025*, pages 8147–8155, 2025.
- [30] Badr AlKhamissi, Greta Tuckute, Antoine Bosselut, and Martin Schrimpf. Brain-like language processing via a shallow untrained multihead attention network. 2024.
- [31] Gavin Mischler, Yinghao Aaron Li, Stephan Bickel, Ashesh D Mehta, and Nima Mesgarani. Contextual feature extraction hierarchies converge in large language models and the brain. *Nature Machine Intelligence*, 6(12):1467–1477, 2024.
- [32] Khai Loong Aw, Syrielle Montariol, Badr AlKhamissi, Martin Schrimpf, and Antoine Bosselut. Instruction-tuning aligns LLMs to the human brain. In *First Conference on Language Modeling*, 2024.
- [33] Zhaofeng Wu, Xinyan Velocity Yu, Dani Yogatama, Jiasen Lu, and Yoon Kim. The semantic hub hypothesis: Language models share semantic representations across languages and modalities. *arXiv preprint arXiv:2411.04986*, 2024.
- [34] Doai Ngo, Mingxuan Sun, Zhengji Zhang, Ashwin G Ramayya, Mark Schnitzer, and Zhe Zhao. Path to intelligence: Measuring similarity between human brain and large language model beyond language task. *arXiv preprint arXiv:2509.08831*, 2025.
- [35] R Quian Quiroga, Leila Reddy, Gabriel Kreiman, Christof Koch, and Itzhak Fried. Invariant visual representation by single neurons in the human brain. *Nature*, 435(7045):1102–1107, 2005.
- [36] R Quian Quiroga, Gabriel Kreiman, Christof Koch, and Itzhak Fried. Sparse but not ‘grandmother-cell’ coding in the medial temporal lobe. *Trends in cognitive sciences*, 12(3):87–91, 2008.
- [37] Moran Cerf, Nikhil Thiruvengadam, Florian Mormann, Alexander Kraskov, Rodrigo Quian Quiroga, Christof Koch, and Itzhak Fried. On-line, voluntary control of human temporal lobe neurons. *Nature*, 467(7319):1104–1108, 2010.
- [38] Matias J Ison, Rodrigo Quian Quiroga, and Itzhak Fried. Rapid encoding of new memories by individual neurons in the human brain. *Neuron*, 87(1):220–230, 2015.
- [39] György Buzsáki. Neural syntax: cell assemblies, synapse ensembles, and readers. *Neuron*, 68(3):362–385, 2010.
- [40] Edmund T Rolls and Alessandro Treves. The neuronal encoding of information in the brain. *Progress in neurobiology*, 95(3):448–490, 2011.
- [41] Lu Hou, Zhiqi Huang, Lifeng Shang, Xin Jiang, Xiao Chen, and Qun Liu. Dynabert: Dynamic bert with adaptive width and depth. *Advances in Neural Information Processing Systems*, 33:9782–9793, 2020.
- [42] Victor Sanh, Thomas Wolf, and Alexander Rush. Movement pruning: Adaptive sparsity by fine-tuning. *Advances in neural information processing systems*, 33:20378–20389, 2020.
- [43] Ofir Zafrir, Ariel Larey, Guy Boudoukh, Haihao Shen, and Moshe Wasserblat. Prune once for all: Sparse pre-trained language models. *arXiv preprint arXiv:2111.05754*, 2021.
- [44] Michael D Fox and Marcus E Raichle. Spontaneous fluctuations in brain activity observed with functional magnetic resonance imaging. *Nature reviews neuroscience*, 8(9):700–711, 2007.
- [45] Gustavo Deco and Maurizio Corbetta. The dynamical balance of the brain at rest. *The Neuroscientist*, 17(1):107–123, 2011.
- [46] An Yang, Anfeng Li, Baosong Yang, Beichen Zhang, Binyuan Hui, Bo Zheng, Bowen Yu, Chang Gao, Chengen Huang, Chenxu Lv, et al. Qwen3 technical report. *arXiv preprint arXiv:2505.09388*, 2025.
- [47] Albert Q. Jiang, Alexandre Sablayrolles, Arthur Mensch, Chris Bamford, Devendra Singh Chaplot, Diego de las Casas, Florian Bressand, Gianna Lengyel, Guillaume Lample, Lucile Saulnier, Léo Renard Lavaud, Marie-Anne Lachaux, Pierre Stock, Teven Le Scao, Thibaut Lavril, Thomas Wang, Timothée Lacroix, and William El Sayed. Mistral 7b, 2023.
- [48] Stephen Merity, Caiming Xiong, James Bradbury, and Richard Socher. Pointer sentinel mixture models. *arXiv preprint arXiv:1609.07843*, 2016.
- [49] Leo Gao, Jonathan Tow, Baber Abbasi, Stella Biderman, Sid Black, Anthony DiPofi, Charles Foster, Laurence Golding, Jeffrey Hsu, Alain Le Noac’h, Haonan Li, Kyle McDonell, Niklas Muennighoff, Chris Ociepa, Jason Phang, Laria Reynolds, Hailey Schoelkopf, Aviya Skowron, Lintang Sutawika, Eric Tang, Anish Thite, Ben Wang, Kevin Wang, and Andy Zou. The language model evaluation harness, 07 2024.

- [50] Alon Talmor, Jonathan Herzig, Nicholas Lourie, and Jonathan Berant. CommonsenseQA: A question answering challenge targeting commonsense knowledge. In *Proceedings of the 2019 Conference of the North American Chapter of the Association for Computational Linguistics: Human Language Technologies, Volume 1 (Long and Short Papers)*, pages 4149–4158, Minneapolis, Minnesota, June 2019. Association for Computational Linguistics.
- [51] Stephanie Lin, Jacob Hilton, and Owain Evans. TruthfulQA: Measuring how models mimic human falsehoods. In *Proceedings of the 60th Annual Meeting of the Association for Computational Linguistics (Volume 1: Long Papers)*, pages 3214–3252, Dublin, Ireland, May 2022. Association for Computational Linguistics.
- [52] Todor Mihaylov, Peter Clark, Tushar Khot, and Ashish Sabharwal. Can a suit of armor conduct electricity? a new dataset for open book question answering. In *EMNLP*, 2018.
- [53] Ankit Pal, Logesh Kumar Umapathi, and Malaikannan Sankarasubbu. Medmcqa: A large-scale multi-subject multi-choice dataset for medical domain question answering. In Gerardo Flores, George H Chen, Tom Pollard, Joyce C Ho, and Tristan Naumann, editors, *Proceedings of the Conference on Health, Inference, and Learning*, volume 174 of *Proceedings of Machine Learning Research*, pages 248–260. PMLR, 07–08 Apr 2022.
- [54] Dan Hendrycks, Collin Burns, Steven Basart, Andy Zou, Mantas Mazeika, Dawn Song, and Jacob Steinhardt. Measuring massive multitask language understanding. *Proceedings of the International Conference on Learning Representations (ICLR)*, 2021.
- [55] Dan Hendrycks, Collin Burns, Steven Basart, Andrew Critch, Jerry Li, Dawn Song, and Jacob Steinhardt. Aligning ai with shared human values. *Proceedings of the International Conference on Learning Representations (ICLR)*, 2021.
- [56] Aida Amini, Saadia Gabriel, Peter Lin, Rik Koncel-Kedziorski, Yejin Choi, and Hannaneh Hajishirzi. Mathqa: Towards interpretable math word problem solving with operation-based formalisms, 2019.
- [57] Wei Huang, Xingyu Zheng, Xudong Ma, Haotong Qin, Chengtao Lv, Hong Chen, Jie Luo, Xiaojuan Qi, Xianglong Liu, and Michele Magno. An empirical study of llama3 quantization: From llms to mllms. *Visual Intelligence*, 2(1):36, 2024.
- [58] Colin Raffel, Noam Shazeer, Adam Roberts, Katherine Lee, Sharan Narang, Michael Matena, Yanqi Zhou, Wei Li, and Peter J. Liu. Exploring the limits of transfer learning with a unified text-to-text transformer. *Journal of Machine Learning Research*, 21(140):1–67, 2020.
- [59] Aakanksha Chowdhery, Sharan Narang, Jacob Devlin, Maarten Bosma, Gaurav Mishra, Adam Roberts, Paul Barham, Hyung Won Chung, Charles Sutton, Sebastian Gehrmann, et al. Palm: Scaling language modeling with pathways. *Journal of Machine Learning Research*, 24(240):1–113, 2023.
- [60] Laurens van der Maaten and Geoffrey Hinton. Visualizing data using t-sne. *Journal of machine learning research*, 9(Nov):2579–2605, 2008.
- [61] Yihe Dong, Lorenzo Noci, Mikhail Khodak, and Mufan Li. Attention retrieves, mlp memorizes: Disentangling trainable components in the transformer. *arXiv preprint arXiv:2506.01115*, 2025.
- [62] Qi Sun, Marc Pickett, Aakash Kumar Nain, and Llion Jones. Transformer layers as painters. In *Proceedings of the AAAI Conference on Artificial Intelligence*, volume 39, pages 25219–25227, 2025.
- [63] Shashank Sonkar and Richard G Baraniuk. Investigating the role of feed-forward networks in transformers using parallel attention and feed-forward net design. *arXiv preprint arXiv:2305.13297*, 2023.
- [64] Shwai He, Guoheng Sun, Zheyu Shen, and Ang Li. What matters in transformers? not all attention is needed. *arXiv preprint arXiv:2406.15786*, 2024.
- [65] Zhenyu Zhang, Ying Sheng, Tianyi Zhou, Tianlong Chen, Lianmin Zheng, Ruisi Cai, Zhao Song, Yuandong Tian, Christopher Ré, Clark Barrett, et al. H2o: Heavy-hitter oracle for efficient generative inference of large language models. *Advances in Neural Information Processing Systems*, 36:34661–34710, 2023.
- [66] Guangxuan Xiao, Yuandong Tian, Beidi Chen, Song Han, and Mike Lewis. Efficient streaming language models with attention sinks, 2024. URL <https://arxiv.org/abs/2309.17453>, 1, 2024.
- [67] Huiqiang Jiang, Yucheng Li, Chengruidong Zhang, Qianhui Wu, Xufang Luo, Surin Ahn, Zhenhua Han, Amir H Abdi, Dongsheng Li, Chin-Yew Lin, et al. Minference 1.0: Accelerating pre-filling for long-context llms via dynamic sparse attention. *Advances in Neural Information Processing Systems*, 37:52481–52515, 2024.
- [68] Aviv Bick, Kevin Li, Eric Xing, J Zico Kolter, and Albert Gu. Transformers to ssms: Distilling quadratic knowledge to subquadratic models. *Advances in Neural Information Processing Systems*, 37:31788–31812, 2024.
- [69] Geoffrey Hinton, Oriol Vinyals, and Jeff Dean. Distilling the knowledge in a neural network. *arXiv preprint arXiv:1503.02531*, 2015.

- [70] Sharath Turuvekere Sreenivas, Saurav Muralidharan, Raviraj Joshi, Marcin Chochowski, Ameya Sunil Mahabaleshwarkar, Gerald Shen, Jiaqi Zeng, Zijia Chen, Yoshi Suhara, Shizhe Diao, et al. Llm pruning and distillation in practice: The minitron approach. *arXiv preprint arXiv:2408.11796*, 2024.
- [71] David R So, Wojciech Manke, Hanxiao Liu, Zihang Dai, Noam Shazeer, and Quoc V Le. Primer: Searching for efficient transformers for language modeling, 2022. URL <https://arxiv.org/abs/2109.08668>.
- [72] Yixin Song, Zeyu Mi, Haotong Xie, and Haibo Chen. Powerinfer: Fast large language model serving with a consumer-grade gpu. In *Proceedings of the ACM SIGOPS 30th Symposium on Operating Systems Principles*, pages 590–606, 2024.
- [73] Keivan Alizadeh, Seyed Iman Mirzadeh, Dmitry Belenko, S Khatamifard, Minsik Cho, Carlo C Del Mundo, Mohammad Rastegari, and Mehrdad Farajtabar. Llm in a flash: Efficient large language model inference with limited memory. In *Proceedings of the 62nd Annual Meeting of the Association for Computational Linguistics (Volume 1: Long Papers)*, pages 12562–12584, 2024.

## A Unstructural Pruning v.s. Structural Pruning

### Setup

Consider a 2-layer ReLU MLP

$$f(x) = W_2 \sigma(W_1 x + b_1) + b_2,$$

with input dimension  $d$ , hidden width  $m$ , output dimension 1 for simplicity, and  $\sigma(z) = \max\{z, 0\}$  applied elementwise.

Let  $W_1 \in \mathbb{R}^{m \times d}$  have rows  $w_1^{(j)} \in \mathbb{R}^d$  (one per hidden unit),  $b_1 \in \mathbb{R}^m$ ,  $W_2 \in \mathbb{R}^{1 \times m}$ , and  $b_2 \in \mathbb{R}$ .

We consider two pruning regimes:

1. **Unstructured (entry-wise) pruning:** Keep width  $m$ , but zero out some entries of  $W_1$  inside each column; no hidden unit is forced to be removed unless an entire column becomes zero.
2. **Structured (column) pruning:** Select a subset  $S \subset [m]$  of size  $m'$  and zero entire columns  $w_1^{(j)}$  and the corresponding  $W_{2,j}$  for  $j \notin S$ . This is equivalent to reducing the width to  $m'$ .

To compare at a fixed 'budget', define

$$\mathcal{F}_{\text{unstruct}}(m, K) := \{f \mid \text{realizable with width } m \text{ and at most } K \text{ nonzeros in } W_1\},$$

$$\mathcal{F}_{\text{struct}}(m', K) := \{f \mid \text{realizable with width } m' \text{ and at most } K \text{ nonzeros in } W_1\}.$$

We will prove:

$$\boxed{\mathcal{F}_{\text{struct}}(m', K) \subsetneq \mathcal{F}_{\text{unstruct}}(m, K) \quad \text{whenever } m' > 0, m > m'.$$

This means: for the same parameter sparsity budget  $K$ , keeping all  $m$  neurons and sparsifying within them yields a strictly larger function class than deleting  $m - m'$  neurons.

### Step 1: Inclusion

Take any  $f \in \mathcal{F}_{\text{struct}}(m', K)$ . Realize it with width  $m'$  and  $\leq K$  nonzeros in  $W_1$ . Embed that network into width  $m$  by adding  $m - m'$  all-zero columns and zeros in the corresponding output weights. This uses the same  $\leq K$  nonzeros in  $W_1$ . Hence  $f \in \mathcal{F}_{\text{unstruct}}(m, K)$ .

Therefore:

$$\mathcal{F}_{\text{struct}}(m', K) \subseteq \mathcal{F}_{\text{unstruct}}(m, K).$$

### Step 2: Strictness via 1D Expressivity

It remains to show the inclusion is *strict*. It suffices to exhibit one function realizable with width  $m$  under the  $K$ -sparsity budget that *cannot* be realized with width  $m' < m$ , regardless of how the same  $K$  nonzeros are allocated.

In the 1D case ( $d = 1$ ) for ReLU nets:

- A width- $q$  2-layer ReLU network can produce at most  $q$  breakpoints, hence at most  $q + 1$  linear pieces.

- Conversely, for any ordered set of  $q$  distinct breakpoints  $\tau_1 < \dots < \tau_q$ , one can realize a continuous piecewise-linear function with those breakpoints using width  $q$  by taking units  $\sigma(x - \tau_j)$  with suitable output weights to match desired slopes.

In 1D, a hidden neuron only needs its scalar weight and bias to place a breakpoint; that is 2 nonzeros per neuron in  $W_1$  and  $b_1$ . Thus, with width  $m$ , using at most  $K = 2m$  nonzeros in  $W_1$ , we can realize a function with exactly  $m$  breakpoints and hence  $m + 1$  linear pieces.

Formally, define

$$g_m(x) = \sum_{j=1}^m a_j \sigma(x - \tau_j) + c,$$

with strictly increasing  $\tau_j$  and nonzero  $a_j$  chosen so each  $\tau_j$  is a genuine breakpoint. Then  $g_m \in \mathcal{F}_{\text{unstruct}}(m, K)$  with  $K = 2m$ .

However, any width- $m'$  2-layer ReLU network has at most  $m'$  breakpoints, so it *cannot* equal  $g_m$  when  $m > m'$ . Therefore:

$$g_m \notin \mathcal{F}_{\text{struct}}(m', K) \quad \text{for all } m' < m.$$

Thus:

$$\mathcal{F}_{\text{struct}}(m', K) \subsetneq \mathcal{F}_{\text{unstruct}}(m, K).$$

### Consequence

Unstructured pruning (keep width  $m$ ) can realize functions with up to  $m$  breakpoints in 1D using just  $2m$  nonzeros in  $W_1$ . Structured pruning to width  $m' < m$  caps you at  $m'$  breakpoints, regardless of how you spend the same number  $K$  of nonzeros.

Therefore, at equal sparsity budget, entry-wise pruning strictly dominates column pruning in expressivity.

## B Why Bias Helps

### B.1 Short Proof

Let  $W \in \mathbb{R}^{d \times n}$ ,  $X \in \mathbb{R}^n$ , and let  $S(X) \in \mathbb{R}^n$  be a (possibly nonlinear) transformation of  $X$ . We aim to approximate the target  $Y := \mathbf{W}X$  using either:

$$\hat{Y}_0 = \mathbf{W}S(X), \quad \hat{Y}_b = \mathbf{W}S(X) + b. \tag{8}$$

**Case 1: Bias  $b = b(X)$  depends on  $X$ .** Choose

$$b(X) = \mathbf{W}X - \mathbf{W}S(X), \tag{9}$$

so that

$$\hat{Y}_b = \mathbf{W}S(X) + b(X) = \mathbf{W}X. \tag{10}$$

Thus, the approximation is exact, and the error is zero.

**Case 2: Constant bias  $b \in \mathbb{R}^d$ .** Let the residual be

$$e(X) = \mathbf{W}X - \mathbf{W}S(X). \tag{11}$$

Define the mean squared error (MSE):

$$\mathcal{L}(b) := \mathbb{E} [\|e(X) - b\|^2]. \tag{12}$$

Expanding gives:

$$\mathcal{L}(b) = \mathbb{E} [\|e(X)\|^2] - 2b^\top \mathbb{E}[e(X)] + \|b\|^2. \tag{13}$$

This is minimized when

$$b^* = \mathbb{E}[e(X)] = \mathbb{E}[\mathbf{W}X - \mathbf{W}S(X)]. \tag{14}$$

Thus, the minimized loss is

$$\mathcal{L}(b^*) = \mathbb{E} [\|e(X)\|^2] - \|b^*\|^2. \tag{15}$$

Hence,

$$\mathcal{L}(b^*) \leq \mathcal{L}(0), \tag{16}$$

with equality if and only if  $\mathbb{E}[e(X)] = 0$ . **Conclusion.** Including a bias term improves approximation by reducing (or eliminating) systematic error in  $\mathbf{W}S(X)$ . Thus,  $\mathbf{W}S(X) + b$  is a better approximation to  $\mathbf{W}X$  than  $\mathbf{W}S(X)$  alone.

## B.2 Improving Generalization

Let:

- $X \in \mathbb{R}^n$ : input vector
- $S(X) \in \mathbb{R}^n$ : transformed input (e.g. nonlinear function)
- $W \in \mathbb{R}^{d \times n}$ : weight matrix
- $b \in \mathbb{R}^d$ : bias vector
- $Y = WX$ : target

We compare two models:

$$f_0(X) = WS(X) \quad (\text{no bias}) \quad f_b(X) = WS(X) + b \quad (\text{with bias})$$

### 1. Approximation Error Reduction

Define the residual:

$$e(X) = WX - WS(X)$$

The optimal constant bias is:

$$b^* = \mathbb{E}[WX - WS(X)] = W(\mathbb{E}[X] - \mathbb{E}[S(X)])$$

Then:

$$f_b(X) = WS(X) + b^* \approx WX$$

This improves the approximation of the true target  $WX$ , especially when  $S$  is nonlinear.

### 2. Generalization and Model Complexity

The hypothesis spaces:

$$\mathcal{H}_0 = \{X \mapsto WS(X)\} \quad \mathcal{H}_b = \{X \mapsto WS(X) + b \mid b \in \mathbb{R}^d\}$$

Adding a bias term increases the expressiveness by only  $d$  parameters (constant w.r.t. input dimension or sample size), so the complexity increase is negligible.

From statistical learning theory, the generalization error is bounded by:

$$\mathcal{E}_{\text{gen}} \leq \mathcal{E}_{\text{train}} + \mathcal{O}\left(\frac{\text{complexity}}{\sqrt{N}}\right)$$

Adding bias:

- Reduces  $\mathcal{E}_{\text{train}}$  (empirical error)
- Only slightly increases complexity
- Thus lowers total generalization error

### 3. Centering and Activation Shift

In practice, even when inputs are zero-centered, nonlinear transformations (in our case is activation sparsification) may shift the mean away from zero. The bias term allows the model to learn this shift explicitly, improving alignment with the target and leading to: 1) *Smaller weight norms*; 2) *Lower complexity*; *Better generalization*.

## C Implementation Details

We use the Wikitext-raw-v2 dataset [48] as calibration data to train the spontaneous neurons. During training, each weight block  $\mathbf{W}$  is associated with a spontaneous activation  $\vec{\alpha}$  (a set of learnable parameters), and we transform these activations into bias terms inside  $\mathbf{W}$ , i.e.,  $\forall \mathbf{W} : \vec{b}_{\mathbf{W}} = \mathbf{W}\vec{\alpha}$ . Once training is complete, the spontaneous activations  $\vec{\alpha}$  become fixed, and treating them as bias terms (referred to as spontaneous neurons) introduces no additional matrix multiplication. This preserves the model’s inference efficiency, as shown in Table 2.

We evaluate the effectiveness of spontaneous neurons on three main LLM backbones: the Llama3 family [5], Mistral-v2-7B [47], and the Qwen3 family [46]. All models share the same training configuration: a learning rate of 1e-5, 10 training epochs, a batch size of 8, and a block size of 128 for dataset chunking. We train all models on four Nvidia A6000 GPUs. For larger models such as Llama3-8B, Mistral-v2-7B, and Qwen3-8B, the training typically takes between 1.14 and 2.25 hours (1.14h for Llama3-8B, 1.85h for Mistral-v2-7B, and 2.25h for Qwen3-8B), while smaller models can be trained in under 20 minutes.

## D Zero-Shot Table

Table 3: Numerical value for zero-shot performance of 3 backbone LLMs on 6 QA tasks. We use  $\uparrow$  to highlight the improve of SPON over TEAL.

Model	Method	CommonsenseQA	MathQA	MedMCQA	MMLU	OpenBookQA	TruthfulQA
Llama3-8b	FULL	77.23%	39.46%	58.93%	68.05%	33.80%	54.03%
	TEAL	68.39%	36.11%	50.08%	59.69%	30.40%	40.14%
	SPON	69.21% $\uparrow$	37.12% $\uparrow$	49.96% $\downarrow$	60.95% $\uparrow$	31.60% $\uparrow$	41.69% $\uparrow$
Mistral-v2-7B	FULL	66.91%	36.92%	46.31%	59.05%	35.60%	66.82%
	TEAL	62.49%	34.67%	44.08%	55.37%	32.80%	57.08%
	SPON	63.47% $\uparrow$	34.81% $\uparrow$	43.56% $\downarrow$	55.78% $\uparrow$	32.80% —	57.15% $\uparrow$
Qwen3-8b	FULL	78.71%	49.61%	59.62%	72.97%	31.00%	54.41%
	TEAL	74.77%	46.03%	52.95%	68.78%	29.60%	52.78%
	SPON	74.28% $\downarrow$	46.70% $\uparrow$	53.41% $\uparrow$	68.79% $\uparrow$	31.80% $\uparrow$	53.59% $\uparrow$